Carbohydrate Polymers 88 (2012) 496–501

Contents lists available at SciVerse ScienceDirect

Carbohydrate Polymers

journal homepage: www.elsevier.com/locate/carbpol

Reinforcement of vulnerable historic silk fabrics with bacterial cellulose film and its light aging behavior

Shun-Qing Wu[a,1], Mei-Ying Li[b,c,1], Bei-Song Fang[a], Hua Tong[b,c,*]

[a] Jingzhou Preservation Centre of Cultural Relics, Jingzhou, 434020, China
[b] College of Chemistry and Molecular Sciences, Wuhan University, Wuhan, 430072, China
[c] Archaeology Research Center of Science and Technology, Wuhan University, Wuhan, 430072, China

ARTICLE INFO

Article history:
Received 24 September 2011
Received in revised form 2 December 2011
Accepted 21 December 2011
Available online 31 December 2011

Keywords:
Bacterial cellulose
Historic silk fabric restoration
Light aging behavior

ABSTRACT

Bacterial cellulose film was used to reinforce the vulnerable historic silk fabrics as a degradable restoration material, instead of the traditionally used synthetic polymers, for the purpose of storage and display. Both historic silk samples and artificial aged (ultraviolet and ozone aging) silk samples were restored with BC. BC restored samples were also artificial aged to investigate the degradation behavior of BC on silk fabrics. The effect of BC reinforcement and the status of BC on the surface of the silk fibers before and after artificial aging were investigated by SEM, ATR-FTIR, XRD, TG and tensile tests. The results showed that crystallinity, thermal stability and tensile strength (increased by 213%) of the silk samples were improved by BC restoration and BC could be degraded with little damage to silk fibers. This work suggests that BC is a promising material for restoration of vulnerable silk fabrics and other such reinforcement applications.

1. Introduction

Silk belongs to one of the most precious and yet the most vulnerable part of Chinese cultural heritage. As early as in the Shang dynasty (B.C. 1600–B.C. 1046) in China, silk reeling technology was already invented and silk fabrics were regarded as a symbol of luxury (Wang, 1990). Due to the long history of silk culture in China, large numbers of valuable and fabulous silk fabrics were discovered in various ancient tombs. Most of the silk fabrics are made of degummed *Bombyx mori* silk which is mainly comprised of fibroin protein fibers. Fibroin is consisted of 18 amino acids (Zuo, Dai, & Wu, 2006) and is lagrely formed from hexapeptide repeat motifs (-Gly-Ala-Gly-Ala-Gly-Ser-) which fold into anti-parallel β-sheets and aggreagte into crystallites. These β-crystallites are embedded in an amorphous matrix formed from the remainder of the protein which is rich in residues with bulky, polar side-chains (Garside & Wyeth, 2007). Determining by the protein composition, many factors including water (Peacock, 1996), microorganism (Seves, Romanò, maifreni, Sora, & Ciferri, 1998), light (Tsuboi, Ikejiri, Shiga, Yamada, & Itaya, 2001; Tsuge, Yokoi, Ishida, Ohtani, & Becker, 2000) and heat (Zhang, Berghe, & Wyeth, 2011) can induce deterioration of silk fabrics and the degradation usually proceeds from the readily accessible, poor ordered amorphous regions which are rich in reactive residues. Thus, undergoing long time of soil burial, many of the historic silk fabrics are in poor physical and chemical condition, some even disintegrated when touched. For the purpose of protection against further degradation and long-term preservation, appropriate protection and restoration methods are desperately demanded.

A wide variety of materials, such as adhesives, polymers, fungicides, deacidifying agents, detergents, solvents, etc., have hitherto been used in conservation of historic textiles (Abdel-Kareem, 2005). Among these, especially polymers, usually synthetic polymers, are widely used as consolidating agents or adhesives in the conservation and restoration of textiles (Coccaa et al., 2006) due to their good mechanical property and good bonding with substrates. But synthetic polymers have potential problems for applications in conservation and restoration of cultural relics considering their irreversible aging behavior. Mechanical and physical properties of polymers deteriorate over time. As minor deterioration accumulates to certain extent, polymers are no longer helpful in protecting and conserving historic textiles and sometimes even lead to side-effects. The problem is that deteriorated synthetic polymers are difficult to remove without damage to the historic silk textiles. Most of the synthetic polymers can only be dissolved in either organic solvent or degraded at extreme condition, such as high temperature, which is harmful for the textile and is not acceptable in cultural relic conservation. Therefore, biopolymers, which feature both

* Corresponding author at: College of Chemistry and Molecular Sciences, Wuhan University, Wuhan, 430072, China. Tel.: +86 027 68764510; fax: +86 027 68752136.
E-mail address: sem@whu.edu.cn (H. Tong).
[1] These two authors contributed equally to this work as co-first authors.

0144-8617/$ – see front matter © 2011 Elsevier Ltd. All rights reserved.
doi:10.1016/j.carbpol.2011.12.033

good mechanical property and degradability, are considered as substitutes for synthetic polymers. As a kind of degradable biopolymer with remarkable mechanical properties (Iguchi, Yamanaka, & Budhiono, 2000) and organic solvent free production method, bacterial cellulose was selected to restore historic silk textiles as an attempt.

Bacterial cellulose (BC) produced by some bacteria, with the molecular formula of BC $(C_6H_{10}O_5)_n$, has a β-1,4 linkage between two glucose molecules (Shoda & Sugano, 2005) and unique physical and chemical features different from plant cellulose, including high purity, high crystallinity, high Young's modulus, excellent biological affinity and biodegradability (Retegi et al., 2010; Putra, Kakugo, Furukawa, Gong, & Osada, 2008). Especially, the estimated value of Young's modulus of BC reaches as high as 114 Gpa (Hsieh, Yano, Nogi, & Eichhorn, 2008). Furthermore, the abundant side groups made it easily to be functionalized. Owing to its excellent properties, BC has been widely used as reinforcement agent for composite applications. For instance, BC has been used as reinforcement agent in glycerol-plasticized cassava starch bionanocomposites and the elastic modulus of the final composite was seventeen times higher than that of the starch matrix (Woehl et al., 2010).

Up to now, BC has not been used on restoration of historic textiles as far as we know. In present study, bacterial cellulose was employed in restoration of historic silk. Due to the rarity and irregular shape of the historic silk fabrics which were not appropriate for large amount of repeated tests, artificial aged silk samples were used as substitutes for restoration experiment first. Ultraviolet (UV) light and ozone treatment was used to prepare artificial aged silk samples (AAS) to produce the proper residual tensile strength which was close to that of the pristine historic silk samples (PHS). Both the AAS and the PHS samples were restored with BC. To investigate the degradation behavior of BC on silk, UV light and ozone treatment was also performed at BC restored silk samples. The effect of BC restoration and the status of BC on the surface of the silk fabrics were characterized by means of scanning electron microscope (SEM), whiteness meter, attenuated total reflection-Fourier transform infrared (ATR-FTIR) spectroscopy, X-ray diffraction (XRD), thermogravimetry (TG) and tensile test.

2. Experimental

2.1. Materials

Historical silk fabrics, excavated from the Han Dynasity tomb in Xiejiaqiao, Hubei, China, were supplied by Jingzhou Preservation Center of Culture Relics (Jingzhou, China). Plain weaved modern natural silk textiles were purchased from Hubei natural Science and Technology Co., Ltd.

2.2. Ultraviolet light and ozone aging of silk samples

Purchased modern natural silk samples were exposed to UV lamps transmitting at 254 nm for 12 d at 50 ± 10 °C and relative humidity was controlled at 55 ± 5%. Ozone flow (300 mg/h) was delivered 0.5 h every 1.5 h. Samples were turned over every 1 h. Obtained artificial aged silk (AAS) samples were used as alternatives of pristine historic silks (PHS) for BC restoration. BC restored artificial aged silk (BC/AAS) samples were treated at the same condition for 12 h and 24 h separately to research their light aging behavior.

2.3. Restoration of silk samples with bacterial cellulose (BC)

AAS and PHS samples were restored with BC in the way described as following: Ace. Xylinum[1.1812], purchased from IMCAS (Institute of Microbiology, Chinese Academy of Sciences, Beijing, China), was cultured in 50 mL of medium containing 2% glucose, 2% peptone, 0.2% citrate acid, 0.27% $Na_2HPO_4{\cdot}12H_2O$, 0.03% $MgSO_4{\cdot}7H_2O$ in a 500 mL flask with shaking at 150 rpm for 72 h at 28 °C. Fermentation medium, containing 10% glucose, 2% yeast extract, 0.5% ethanol, 0.1% citrate acid, 0.2% $Na_2HPO_4{\cdot}12H_2O$, 0.1% KH_2PO_4, 0.02% $MgSO_4{\cdot}7H_2O$ was inoculated with homogenized Ace. Xylinum culture in ratio of 10:1. Obtained mixture was sprayed onto silk samples until they were entirely soaked. The soaked silk samples were cultured at 30 °C and 90% relative humidity (RH) for about 15 h. Obtained samples were heated at around 60 °C for 1 h to inactivate the bacteria cells, washed thoroughly with deionized water to remove the bacteria cells and adsorbed medium and air dried. Detailed parameters of the bacteria strain and the restored samples were listed in Table 1.

Table 1
Parameters of the bacteria strain and restored silk samples.

Bacteria strain	Average productivity (g/L)	Weight ratio of BC in BC/silk samples (%)
Ace. Xylinum[1.1812]	6.63	11.79

2.4. Characterization

The total color change (ΔE) of the samples was measured using a whiteness meter (Qingtong YQ-Z-48A, China) with diffuse reflectance method. Scanning electron microscope (SEM) images of samples were observed with a FEI Quanta 200 scanning electron microscope at 30 keV accelerating voltage. Samples were mounted on an aluminum stub and sputtered with aurum before observed. ATR-FTIR spectra were recorded using a Fourier transform infrared spectroscopy (NICOLET 5700, USA) equipped with an ATR-Omni attachment. Spectra over the range 4000–700 cm^{-1} were collected with a resolution of 4 cm^{-1}. X-ray diffraction (XRD) of samples was performed by a Rigaku D/Max-3C diffractometer with Cu Kα radiation from a source operated at 40 kV and 80 mA. Diffraction was measured in reflection mode at scanning rate of 2°/min. Thermogravimetry (TG) was performed on samples under oxidizing condition. Samples were heated in diamond TG–DTA analyzer until completely decomposed in an aluminum crucible at a heating rate of 15 °C/min. The flow rate of purge gas (air) was 20 mL/min. Tensile tests were performed in a mechanical testing machine (Qingtong WZL-30, Hangzhou) using a 30 N load cell. Test samples were cut in 15 cm × 1.5 cm. The crosshead rate used in the test was 5 mm/min. Tensile strength was calculated by

$$S = \frac{F}{L_w}$$

where F was the ultimate breaking force determined by the machine and L_w was the width of the test sample.

3. Results and discussion

3.1. Appearance and morphology

An important principle in the conservation of cultural relics is to retain the appearances as what they were. As shown in Fig. 1, the appearances of PHS (Fig. 1a) and AAS (Fig. 1c) were well preserved in the BC/PHS (Fig. 1b) and the BC/AAS (Fig. 1d) separately except that the colors turned a little pale. In order to quantitatively evaluate the influence of BC restoration on color, chromatic values of all the samples mentioned were determined. The results shown in Table 2 suggested that the color differences ΔE caused by BC restoration were less than 1.00, which was acceptable in the conservation of historic textiles. Moreover, something noticeable was

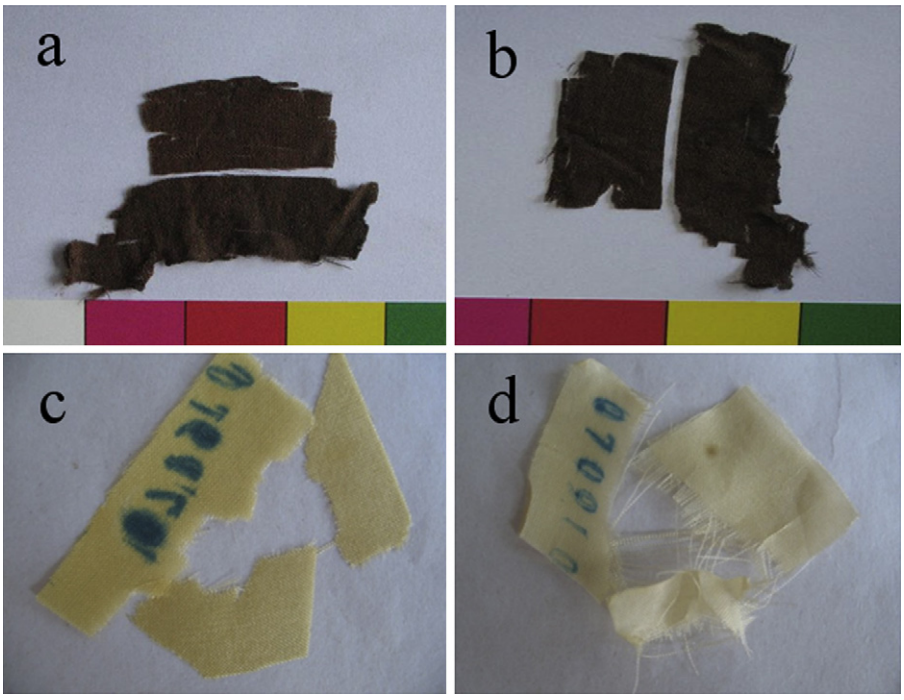

Fig. 1. Photographs of (a) PHS, (b) BC/PHS, (c) AAS and (d) BC/AAS.

displayed in Fig. 1c and d. Both the AAS and the BC/AAS could be easily torn apart, but the fractures were different. For the AAS, the fracture was clean and no extending fibers were observed. For the BC/AAS, extending fibers were obvious around the fracture, suggesting the enhanced mechanical properties after BC restoration.

In order to investigate the morphology of BC on the surface of silk fiber and the state of interface adhesion between BC and silk fibers, electron scanning microscope images of the cross sections of the samples were observed. As shown in Fig. 2, the surface of AAS (Fig. 2a) was smooth and clean and the surface of BC/AAS (Fig. 2b) was enwrapped by a clearly seen rough film. The compatibility between the film and the silk fibers was good and no obvious phase interface was observed (Fig. 2c). Besides, the adjacent fibers were tightly bound up by the BC coating, which might contribute to the enhanced mechanical property. When the BC/AAS was subjected to UV light and ozone for 12 h (BC/AAS-12, Fig. 2d), the rough coating disappeared and some threadlike residues left on the surface and connected the adjacent silk fibers. With the aging time up to 24 h (BC/AAS-24, Fig. 2e), the threadlike residues almost completely disappeared and the surfaces of the silk fibers were as smooth as AAS.

3.2. FT-IR spectroscopy

ATR FT-IR spectroscopy was employed to confirm the existence of bacterial cellulose in the restored silk samples and analyze its effect on silk protein conformation at molecular level. Results manifested in Fig. 3 showed that the main peaks in the fingerprint region for all the samples were nearly the same, which meant that the BC restoration did not change the silk protein conformation. The main difference existed in the region 3500–2600 cm^{-1}. Compared to AAS and PHS, the characteristic absorption bands of BC at 2922 cm^{-1} and 2851 cm^{-1} assigned to C—H stretching vibrations (Chen, Shen, Yu, Hu, & Wang, 2010; Barud et al., 2008; Kondo & Sawatari, 1996) appeared in the spectra of BC/AAS and BC/PHS, which proved that the film that enwrapped the silk fibers was composed of BC. After ultraviolet light aging, the intensities of the peaks at 2922 cm^{-1} and 2851 cm^{-1} decreased with the aging time. In the spectrum of BC/AAS-24, the absorption bands of BC nearly disappeared. While the other absorption bands remained the same as AAS. The results suggested that the BC on the surface of BC/AAS degraded and the degree increased over the aging time while the structure of AAS was retained.

Another difference worth noticing was the change of the peak in the region 3400–3200 cm^{-1} assigned to N—H stretching vibrations of silk fibroin protein and O—H stretching vibrations of BC. This peak was sensitive to hydrogen bond (Sargunamani & Selvakumar, 2006; Monti, Taddei, Freddi, Ohgo, & Asakura, 2003), thus its change could reflect the change of hydrogen bonding environment. Compared to AAS, the intensity of this peak obviously increased due to the increase in —OH content of BC in the spectrum of BC/AAS. Meanwhile, the profile became sharper and the peak location shifted from 3271 cm^{-1} to 3279 cm^{-1}, implying the existence of the interface interactions between the BC restoration coating and the silk fibers which changed the hydrogen bonding environment in BC/AAS. In the spectra of BC/AAS-12 and BC/AAS-24, the intensity of the peak decreased with the decrease of —OH of BC. The location remained at around 3279 cm^{-1} and the profile broadened with the increase of aging time, indicating that the interactions between the BC coating and the silk fibers weakened with the process of BC degradation. These interactions might be attributed to the hydrogen bonds formed between the hydroxyl groups of BC and the amido groups or the amino acid residues of silk protein fibers.

Table 2
Color differences and tensile strengths of the silk samples.[a]

Samples	ΔE	Tensile strength (N/m)
AAS	40.03 ± 0.19	40 ± 8
BC/AAS	39.29 ± 0.18	125 ± 11
BC/AAS-12	58.71 ± 1.62	45 ± 11
BC/AAS-24	59.08 ± 0.13	36 ± 9
PHS	–	36 ± 1
BC/PHS	–	48 ± 1

[a] Each result was reported as mean value of $n = 9$ measurements except PHS and BC/PHS. For PHS and BC/PHS, $n = 3$.

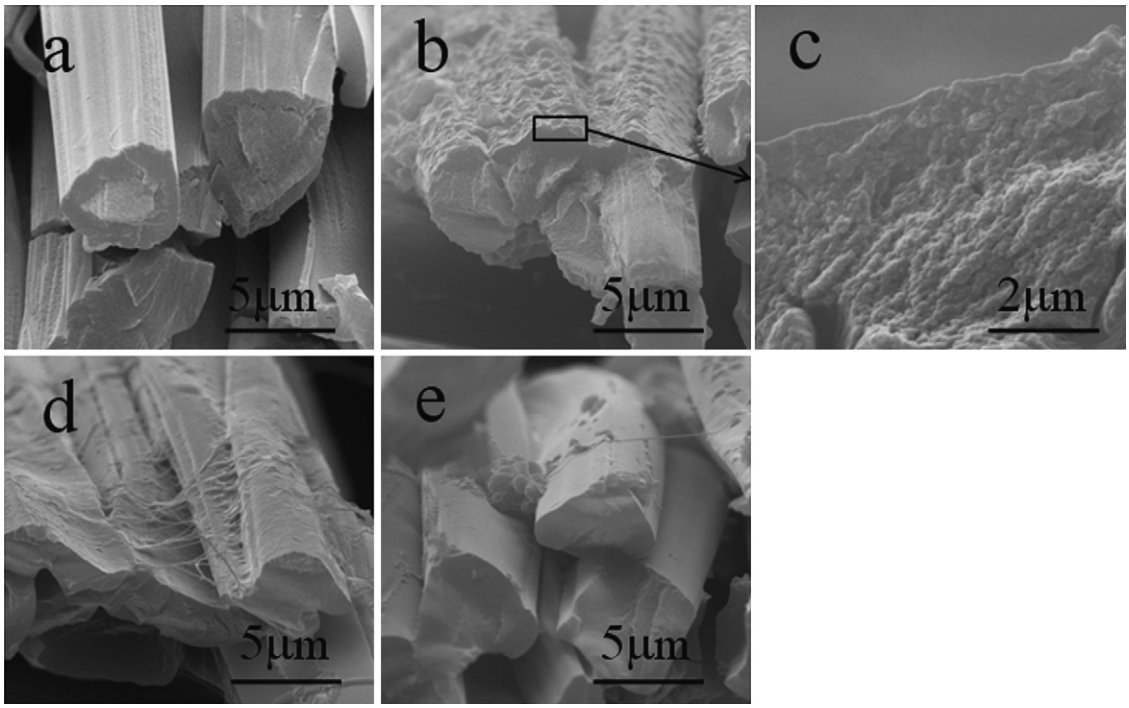

Fig. 2. SEM images of the cross sections of (a) AAS and (b) BC/AAS, (c) the enlarged interface between BC and AAS, and the cross sections of (d) BC/AAS-12 and (e) BC/AAS-24.

3.3. X-ray diffraction analysis

X-ray diffraction analysis was used to characterize the crystalline structure of all the samples. Generally, there have been two types of crystalline structure proposed for silk, silk I and silk II (Feng, Zhou, Zhu, & Chen, 2010). The diffractogram of AAS displayed in Fig. 4 showed the characteristic diffraction peaks at around 9.4° and 20.7° which were attributed to silk II form which corresponded to antiparallel β-sheet crystalline structure with high orientation (Xu, Ke, & Peng, 2006; Yuan, Yao, Chen, Huang, & Shao, 2010) and a shoulder peak at around 24.5° which corresponded to silk I form with lower ratio of β-sheet crystalline structure (Jiang et al., 2007). The PHS displayed an irregular broad peak centered at around 19°, indicating that degradation had proceeded from the amorphous area to the crystalline area of PHS. Both BC/AAS and BC/PHS showed main diffraction peaks of at 20.7° which were significantly stronger and sharper than those of AAS and PHS, implying that the crystallinities of AAS and PHS were increased by BC restoration. But the characteristic peaks of BC at 16.5° and 22.5° (Barud et al., 2008; Retegi et al., 2010) were not observed as predicted. It might be explained that BC was induced to crystallize with *d*-spacing of 4.29 Å by silk fiber template during the restoration process and contributed to the enhanced peak at 20.7°. Thus with the degradation of BC which featured high crystallinity, the peaks at 20.7° in the diffractograms of BC/AAS-12 and BC/AAS-24 obviously decreased, i.e. the crystallinities decreased.

3.4. Thermal stability

Thermogravimetry analysis was carried out to assess the thermal stability of the silk samples. As shown in Fig. 5, the early minor weight loss observed at initial low temperature (from 30 to 100 °C)

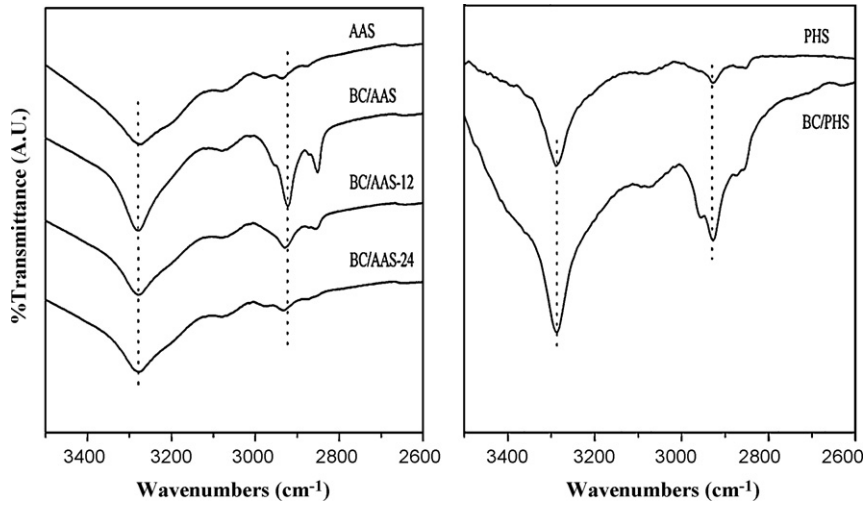

Fig. 3. ATR-FTIR spectra of the silk samples.

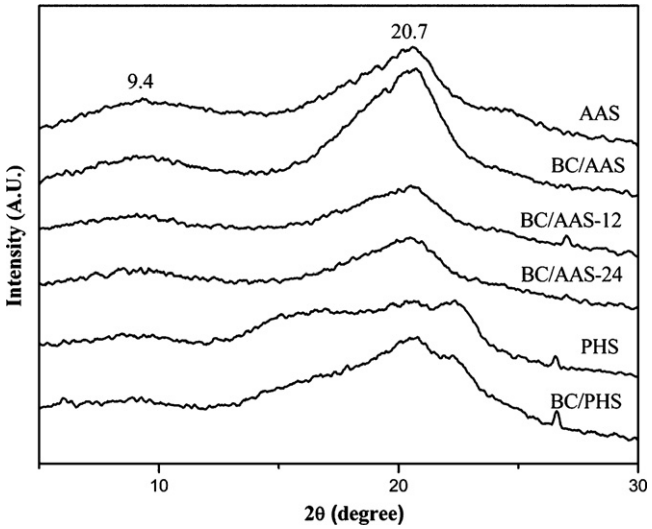

Fig. 4. XRD diffractograms of the silk samples.

for all samples was attributed to the evaporation of absorbed moisture (Gao et al., 2010; Motta, Fambri, & Migliaresi, 2002). Physically adsorbed and hydrogen bond linked water molecules were lost at this stage. AAS showed an onset of degradation at 252 °C and degraded in two main steps with maximum rates of mass loss at 312 and 562 °C, respectively, and the onset of degradation of the BC/AAS increased to 281 °C and the maximum rates of mass loss occurred at 315 and 627 °C. The thermal stability of AAS was obviously increased. Compared with BC/AAS, the onsets of degradation of BC/AAS-12 and BC/24 decreased to 277 and 268 °C separately. The first degradation steps of BC/AAS-12 and BC/AAS-24 were nearly the same as BC/AAS and the maximum mass loss rates of the second step occurred at 522 and 504 °C, respectively, implying that the thermal stability decreased with the degradation of BC. In the case of PHS, the onset of degradation was changed from 311 to 317 °C and the temperature at which the maximum mass loss rate occurred was changed from 495 to 525 °C by BC restoration. The residual mass might be contributed to the contamination which filtered into the historic silk fabrics. Overall, it could be clearly seen from Fig. 5 that BC restoration affected the onset of the first step of degradation and the process of the second degradation step.

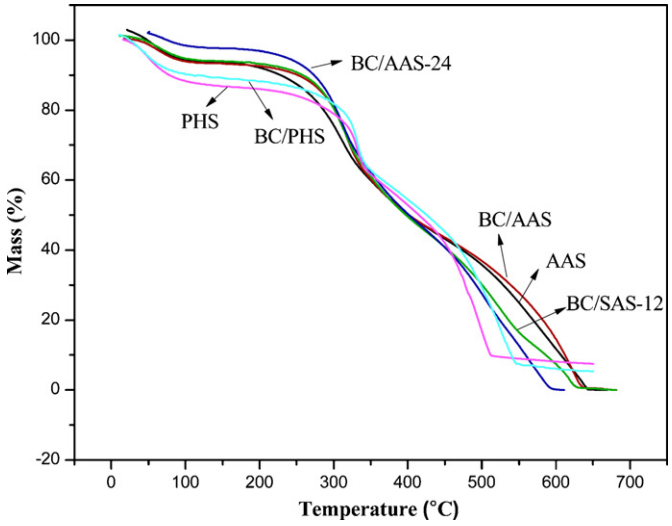

Fig. 5. TG results of the silk samples.

3.5. Tensile test

Effect of BC restoration on mechanical properties was assessed by tensile test. As listed in Table 1, the average tensile strengths of AAS and PHS were 40 N/m and 36 N/m, separately. With BC restoration, the average tensile strengths of BC/AAS and BC/PHS reached 125 N/m and 48 N/m, increased by 213% and 33%, respectively. Compared to BC/AAS, the tensile strengths of BC/AAS-12 and BC/AAS-24 decreased to 45 N/m and 36 N/m, separately.

The trend of the change of tensile strength was coincident with the change of the residual BC on the surface of silk fibers displayed in SEM images (Fig. 2), the change of interactions between BC and silk fibers illustrated in FT-IR spectrum (Fig. 3) and the change of crystallinity as illustrated in XRD diffractograms (Fig. 4). This finding suggested that the mechanical property of the BC/silk fiber composite was related to the quantum of BC on silk fibers, the interactions between BC coating and silk fibers and the crystallinity of the composite. It could be explained as following. First, it was understandable that the interactions between BC coating and silk fibers were significant as the stiffness and strength of a composite material relies on the interaction between the matrix and the reinforcement (Quero et al., 2010). Second, the more BC there were, the more interactions were generated, thus the stronger the BC/silk composite was. Finally, it was acknowledged that the increase of crystallinity of a fiber usually led to an improved mechanical property.

In conclusion, the gain in mechanical performance of AAS and PHS by BC restoration could be explained as following: The good compatibility between silk fiber and BC coating made the mechanical energy able to transfer between silk fiber and BC coating and made it able to make use of the high crystallinity and the high elastic modulus of BC film when under tensile stress.

4. Conclusions

BC was used to restore vulnerable historic silk fabrics as degradable reinforcement instead of traditionally used synthetic polymers and the appearances of all the samples were well preserved. Due to the abundant hydroxyl side groups and the high crystallinity and elastic modulus of BC, good interface interactions between BC and silk matrix were formed and the crystallinity, the thermal stability and the tensile strength of the restored sample were improved. The UV light and ozone aging test of restored samples showed that BC could be removed from silk samples with little damage to the fiber's original properties. Therefore, as a degradable, environment friendly and solvent free material with abundant resources, BC is promising in silk fabric restoration and other such reinforcement applications.

Acknowledgement

Financial support of this research from the Key Projects in the National Science & Technology Pillar Program of China during the 11th five-year Plan Period (2006BAK20B02) is gratefully acknowledged.

References

Abdel-Kareem, O. M. A. (2005). The long-term effect of selected conservation materials used in the treatment of museum artefacts on some properties of textiles. *Polymer Degradation and Stabilility*, *87*(1), 121–130.

Barud, H. S., Assunção, R. M. N., Martines, M. A. U., Dexpert-Ghys, J., Marques, R. F. C., Messaddeq, Y., et al. (2008). Bacterial cellulose–silica organic–inorganic hybrids. *Journal of Sol–Gel Science and Technology*, *46*(3), 363–367.

Chen, S. Y., Shen, W., Yu, F., Hu, W. L., & Wang, H. P. (2010). Preparation of amidoximated bacterial cellulose and its adsorption mechanism for Cu^{2+} and Pb^{2+}. *Journal of Applied Polymer Science*, *117*(1), 8–15.

Coccaa, M., D'Arienzo, L., D'Orazio, L., Gentile, G., Mancarella, C., Martuscelli, E., et al. (2006). Water dispersed polymers for textile conservation: A molecular, thermal, structural, mechanical and optical characterization. *Journal of Cultural Heritage*, *7*(4), 236–243.

Feng, X. X., Zhou, L., Zhu, H. L., & Chen, J. Y. (2010). Study on the properties of nano-TiO_2 particles modified silk fibroin porous film. *Journal of Applied Polymer Science*, *116*(1), 468–472.

Gao, C., Xiong, G. Y., Luo, H. L., Ren, K. J., Huang, Y., & Wan, Y. Z. (2010). Dynamic interaction between the growing Ca–P minerals and bacterial cellulose nanofibers during early biomineralization process. *Cellulose*, *17*, 365–373.

Garside, P., & Wyeth, P. (2007). Crystallinity and degradation of silk: Correlations between analytical signatures and physical condition on ageing. *Applied Physics A Materials Science & Processing*, *89*, 871–876.

Hsieh, Y.-C., Yano, H., Nogi, M., & Eichhorn, S. J. (2008). An estimation of the Young's modulus of bacterial cellulose filaments. *Cellulose*, *15*, 507–513.

Iguchi, M., Yamanaka, S., & Budhiono, A. (2000). Bacterial cellulose—a masterpiece of nature's arts. *Journal of Materials Science*, *35*, 261–270.

Jiang, C. Y., Wang, X. Y., Gunawidjaja, R., Lin, Y-H., Gupta, M. K., Kaplan, D. L., et al. (2007). Mechanical properties of robust ultrathin silk fibroin films. *Advanced Functional Materials*, *17*(13), 2229–2237.

Kondo, T., & Sawatari, C. (1996). A Fourier transform infra-red spectroscopic analysis of the character of hydrogen bond in amorphous cellulose. *Polymer*, *37*(3), 393–399.

Monti, P., Taddei, P., Freddi, G., Ohgo, K., & Asakura, T. (2003). Vibrational ^{13}C-cross-polarization/magic angle spinning NMR spectroscopic and thermal characterization of poly(alanine-glycine) as model for silk I *Bombyx mori* fibroin. *Biopolymers*, *72*(5), 329–338.

Motta, A., Fambri, L., & Migliaresi, C. (2002). Regenerated silk fibroin films: Thermal and dynamic mechanical analysis. *Macromolecular Chemistry and Physics*, *203*(10–11), 1658–1665.

Retegi, A., Gabilondo, N., Peña, C., Zuluaga, R., Castro, C., Gañan, P., et al. (2010). Bacterial cellulose films with controlled microstructure–mechanical property relationships. *Cellulose*, *17*(3), 661–669.

Peacock, E. E. (1996). Biodegradation and characterization of water-degraded archaeological textiles created for conservation research. *International Biodeterioration & Biodegration*, *38*(1), 49–59.

Putra, A., Kakugo, A., Furukawa, H., Gong, J. P., & Osada, Y. (2008). Tubular bacterial cellulose gel with oriented fibrils on the curved surface. *Polymer*, *49*(7), 1885–1891.

Quero, F., Nogi, M., Yano, H., Abdulsalami, K., Holmes, S. M., Sakakini, B. H., et al. (2010). Optimization of the mechanical performance of bacterial cellulose/poly(L-lactic) acid composites. *Applied Materials & Interfaces*, *2*(1), 321–330.

Sargunamani, D., & Selvakumar, N. (2006). A study on the effects of ozone treatment on the properties of raw and degummed mulberry silk fabrics. *Polymer Degradation and Stability*, *91*(11), 2644–2653.

Seves, A., Romanò, M., maifreni, T., Sora, S., & Ciferri, O. (1998). The microbial degradation of silk: A laboratory investigation. *International Biodeterioration & Biodegration*, *42*(4), 203–211.

Shoda, M., & Sugano, Y. (2005). Recent advances in bacterial cellulose production. *Biotechnology and Bioprocess Engineering*, *10*(1), 1–8.

Tsuboi, Y., Ikejiri, T., Shiga, S., Yamada, K., & Itaya, A. (2001). Light can transform the secondary structure of silk protein. *Applied Physics A Materials Science & Processing*, *73*(5), 637–640.

Tsuge, S., Yokoi, H., Ishida, Y., Ohtani, H., & Becker, M. A. (2000). Photodegradative changes in chemical structures of silk studied by pyrolysis—gas chromatography with sulfur chemiluminescence detection. *Polymer Degradation and Stability*, *69*(2), 223–227.

Wang, X. (1990). An overview of the development of silk in ancient China. *Academic Journal of Suzhou University*, *3*, 92–102, in Chinese.

Woehl, M. A., Canestraro, C. D., Mikowski, A., Sierakowski, M. R., Ramos, L. P., & Wypych, F. (2010). Bionanocomposites of thermoplastic starch reinforced with bacterial cellulose nanofibers: Effect of enzymatic treatment on mechanical properties. *Carbonhydrate Polymers*, *80*(3), 866–873.

Xu, W. L., Ke, G. Z., & Peng, X. Q. (2006). Studies on the effects of the enzymatic treatment on silk fine powder. *Journal of Applied Polymer Science*, *101*(5), 2967–2971.

Yuan, Q. Q., Yao, J. R., Chen, X., Huang, L., & Shao, Z. Z. (2010). The preparation of high performance silk fiber/fibroin composite. *Polymer*, *51*(21), 4843–4849.

Zhang, X. M., Berghe, I. V., & Wyeth, P. (2011). Heat and moisture promoted deterioration of raw silk estimated by amino acid analysis. *Journal of Cultural Heritage*, doi:10.1016/j.culher.2011.03.002

Zuo, B., Dai, L., & Wu, Z. (2006). Analysis of structure and properties of biodegradable regenerated silk fibroin fibers. *Journal of Materials Science*, *41*, 3357–3361.